Scientific Research Publishing

Advances in Chemical Engineering and Science, 2025, 15(1), 1-16
https://www.scirp.org/journal/aces
ISSN Online: 2160-0406
ISSN Print: 2160-0392

Novel Synthesis and Characterization of Cellulose Nanocrystals Composites Fabricated from Rice Husks

Antonate Wanyonyi, Godfrey Okumu Barasa*, John Onyango Agumba, Samwel Onyango Okoth, Edwin Atego

Department of Physical Sciences, Jaramogi Oginga Odinga University of Science and Technology, Bondo, Kenya
Email: *gobarasa@jooust.ac.ke

How to cite this paper: Wanyonyi, A., Barasa, G.O., Agumba, J.O., Okoth, S.O. and Atego, E. (2025) Novel Synthesis and Characterization of Cellulose Nanocrystals Composites Fabricated from Rice Husks. *Advances in Chemical Engineering and Science*, **15**, 1-16.
https://doi.org/10.4236/aces.2025.151001

Received: August 19, 2024
Accepted: November 24, 2024
Published: November 27, 2024

Abstract

Nanotechnology has shown interest in the utilization of agricultural byproducts as a source for nanostructured materials. Due to their distinctive chemical, thermal, mechanical, morphological, optical, and electrical properties, cellulose nanocrystals (CNCs) have often found utility in a variety of fields. Using sulphuric acid with a 64% weight-to-weight ratio, we managed to extract CNCs chemically from rice husks for the study and examined the effects of varying the hydrolysis period and synthesized composites on optical and thermal characteristics. The usual procedure for preparation was followed, but set the hydrolysis time for 40, 60 and 90 minutes, and also varied temperature at 40˚C, 45˚C and 50˚C. Tonic water and silver nanoparticles were used to synthesize the composites at different ratios. The samples were characterized using UV-Vis spectroscopy, Fourier transform infrared (FTIR) spectroscopy, thermogravimetric analysis (TGA) and differential scanning calorimetry (DSC) techniques. From the results of this study, maximum absorption is observed to shift to shorter wavelengths with an increase in temperature, and the peak absorbance (maximum wavelength) generally increased with hydrolysis time at all three temperatures. The FTIR spectrum of cellulose nanocrystals (CNCs), AgNPs and their composites exhibited distinctive absorption bands indicative of their molecular structure and chemical composition. From the TGA findings, the two composites had a relatively low thermal stability, hence restricting their application to a fixed temperature and below. Additionally, this property makes the composite easily formable into intricate designs, which is ideal for use in optical components and sensors. The low melting point also facilitates recycling and reprocessing, enhancing sustainability by enabling the reuse of the material in various applications. Moreover, the composite's sensitivity to temperature can be useful in temperature-sensing

applications, where changes in its properties at lower temperatures can provide valuable optical feedback.

Keywords

Cellulose Nanocrystals, Nanocomposites, Silver Nanoparticles, Optical Analysis, Thermal Analysis, Rice Husks

1. Introduction

The search for materials for novel and emerging applications is a concern for many researchers and organizations [1]. Therefore, to satisfy this increasing trend, renewable and environmentally sustainable resources need to be exploited. In recent years, cellulose has attracted great interest owing to its unique characteristics, such as abundant availability in nature, renewable, environmentally friendly, biocompatibility, and cost-effective reinforcement of composites [2]. The enhanced properties will enable the composites to be tailored for specific roles. In the past ten years, researchers' interest in nanocellulose and its use as a reinforcing component in nanocomposites has increased because of the material's amazing mechanical reinforcement characteristics, great biodegradability, and ecologically favorable makeup.

Therefore, these characteristics must be managed to improve the interaction between the filler and matrix in order to produce nanocomposites with exceptional and tailored qualities. Understanding the temperature behavior of nanocellulose is crucial, particularly when creating composites of nanocellulose and polymers [3]. The simple synthesis of nanoparticles utilizing natural reducing and stabilizing agents is now possible based on recent research. AgNPs exhibit distinct optical and thermal characteristics that allow them to interact strongly with particular light wavelengths, as demonstrated by the UV-vis spectroscopy used to characterize them. In AgNPs, where electrons can freely flow, the conduction and valence bands are relatively close to one another [4]. As a result, the characteristics of cellulose nanocrystals are modified for use in various domains by the composite created by silver NPs. The composite formed of silver nanoparticles will be useful in a variety of industries, including sensors, wound healing, high-performance textiles, batteries, films, and food packaging. Quinine has also been used widely in the synthesis of compo due to its excellent fluorescence capabilities, and quinine is also utilized to create CNCs composites [5].

2. Experimental

2.1. Characterization of Cellulose Nanocrystals Composite

2.2.1. FTIR Spectroscopy

The broad spectrum ranges from 400 - 4000 cm^{-1} against % transmittance. The technique is used to obtain an infrared spectrum of absorption or emission of

solid, gas, or liquid. The resulting signal at the detector is a spectrum representing a molecular fingerprint of the sample, and different chemical structures produce different fingerprints. It can be used to identify the fundamental groups present in the compound. FTIR spectroscopy was preferred because it doesn't destroy the sample, it is significantly faster than older techniques and more sensitive and precise [6].

2.2.2. UV-Vis Spectroscopy

This is a technique used to study the intensity of light as a function of wavelength using a spectrophotometer. It uses the principle of the Beer-Lamberts Law, where incident light beam is diffracted into a spectrum of wavelength and the dictated intensities displayed in graphs [7]. The spectrophotometer uses tungsten and hydrogen deuterium lamps as the light source as they cover a hole UV-Vis region ranging from 200 - 900 nm. The monochrometer selects the wavelength at which an absorption measurement is made. The photodiode detector is used in the photoconductive mode to convert the light that is transmitted through the sample cell to a signal current [8].

2.2.3. TGA and DSC Spectroscopy

This technique has been widely used to determine the thermal stability of the samples in relation to temperature and mass loss. Using the TGA/DSC machine, we can probe changes in the sample mass from room temperature of about 24˚C up to 1000˚C. Within this range, several changes occur that would result in mass loss, for example, loss of solvent or moisture content through evaporation, thermal decomposition or pyrolysis, which will show decomposition steps [9]. The combination of the two DSC and TGA holds great promise as a tool for unravelling the mechanism of physical and chemical processes that occur during solids degradation.

2.2.4. Pretreatment of Rice Husks

Rice husks were ground into fine powder using the grinding machine. 100 g of this powder was dispersed in 500 ml of distilled water, stirred for 10 minutes at room temperature of 24 degrees Celsius and filtered, then dried at 100 degrees Celsius. This procedure was repeated once more.

2.2.5. Delignification

The residue was then dispersed in 500 ml of a 12% NaOH solution and the suspension stirred for 3 hours at 80˚C. The alkali treated fibres were filtered and washed with distilled water. After the washing, the alkaline treatment was repeated once more and the fibers were dried at 50˚C for 24 hours.

2.2.6. Bleaching

Partial delignification was performed in order to facilitate further whisker extraction. 5 g of dried pre-heated fibers was heated between 60˚C to 70˚C in 150 ml of NaOCL solution (sodium hypochlorite). For stronger bleaching, this procedure was repeated twice using same conditions [10].

2.2.7. Hydrolysis

The bleached fibers samples were heated in a concentrated sulfuric acid solution 64% w/w sulfuric acid in water at 45˚C, 40˚C and 50˚C. The ratio of fiber to acid solution was taken as 1:10 g/ml [11]. In order to compare both treatments, hydrolysis was performed for 40, 60 and 90 minutes under constant stirring. After treatment, the hydrolyzed cellulose samples were washed four times, separating the crystals from the solution. After hydrolysis, the sample was then diluted in cold water at about 5˚C to stop the reaction of sulphuric acid [12]. The sample was continuously dialyzed against water for three days until constant PH was reached. The sample was dialyzed in distilled water so as to remove any free acid molecules.

2.2.8. Silver Nanoparticles and CNC Composite Synthesis

Fresh and healthy aloe Vera leaves were rinsed thoroughly with tap water, followed by distilled water. The leaves were dried at room temperature to remove the water from the surface. They were cut into small pieces. 10 g of finely incised leaves were put into a 250 ml flask containing 100 ml of distilled water and boiled at 80˚C for 1 hour. After cooling, the mixture was centrifuged at 12,000 rmp for 15 min and filtered. Aqueous solution of 1 Mol Silver Nitrate was prepared by dissolving 0.3 mol silver nitrate in 20 ml of deionized water in a 250 volumetric flask. 20 ml of aloe vera leaf extract was mixed with 20 ml of aqueous solution of 1 M Silver Nitrate under vigorous stirring for 30 minutes at room temperature. The mixture was heated at a temperature of between 50˚C and 60˚C and then gradually cooled, filtered and washed with deionized water and will be incubated in a dark place overnight at room temperature [13]. Similarly, the CNC composite was synthesized by mixing CNCs and AgNPs and Quinine in the ratio 1:1, 1:3, 1:4, 2:1, 3:1, 4:1 in distilled water.

3. Results and Discussions

3.1. FTIR Analysis

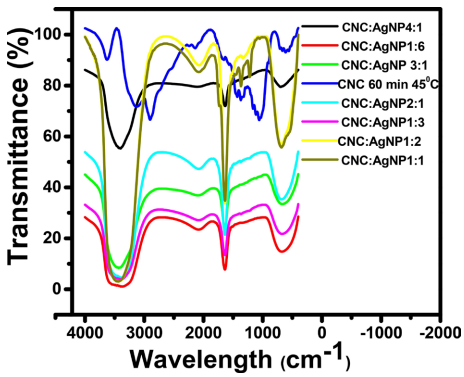

Figure 1. FTIR spectra for CNC and its composite.

The FTIR spectrum of cellulose nanocrystals (CNCs) exhibits distinctive absorption bands indicative of their molecular structure and chemical composition. The prominent peak observed at 3623 cm^{-1} corresponds to the stretching vibration

of hydroxyl (O-H) groups within the cellulose molecules, underscoring the presence of extensive hydrogen bonding among neighboring chains [14]. This intermolecular interaction is crucial for the structural integrity and stability of CNCs [15]. Furthermore, the peaks at 1370 cm^{-1} and 1050 cm^{-1} signify the bending vibrations of C-H bonds and the stretching vibrations of C-O bonds, respectively, further characterizing the chemical composition of CNCs [16]. Finally, [17] provides insights into the integrity of the cellulose backbone in CNCs. The FTIR peaks observed for cellulose nanocrystals (CNCs) and silver nanoparticles (AgNPs) offer insights into their respective molecular structures and compositions. The peak at 3404 cm^{-1}, prominent in CNCs, signifies the stretching vibration of hydroxyl (OH) groups within the cellulose molecules, indicative of strong hydrogen bonding among adjacent chains [17]. Conversely, in AgNPs, the absence of this peak suggests a different chemical composition or surface functionalization. The peak at 2106 cm^{-1}, observed in both CNCs and AgNPs, may correspond to different vibrational modes. In CNCs, this peak could represent the asymmetric stretching vibration of sulfate (SO_4) groups introduced during the sulfuric acid hydrolysis process, enhancing their dispersibility in aqueous solutions, as discussed by Eichhorn *et al.* (2010). In AgNPs, this peak could be associated with the stretching vibration of chemical bonds involving silver atoms or surface ligands. The peak at 1620 cm^{-1} in AgNPs might correspond to the stretching vibration of carbonyl (C=O) groups or other functional groups present in stabilizing agents or capping ligands on the nanoparticle surface. Additionally, the peak at 650 cm^{-1} in AgNPs could be attributed to the stretching vibration of silver-sulfur (Ag-S) bonds, if present, indicating interactions between silver atoms and sulfur-containing molecules, such as thiols or sulfides. (**Figure 1**)

3.2. UV-Vis Spectroscopy

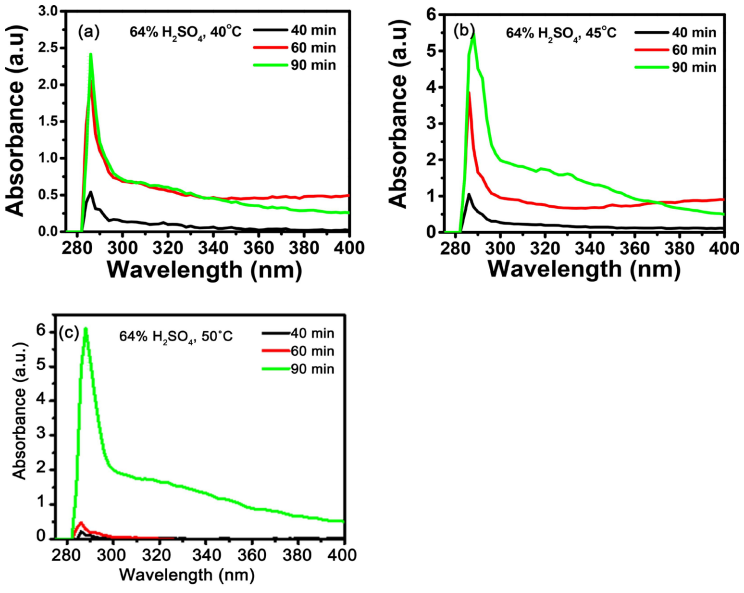

Figure 2. Absorbance spectra for CNC for time dependence.

Table 1. Position of peaks of time dependent absorption of CNC.

Temperature	Hydrolysis time	Peak (maximum wavelength)
40˚C	40 minutes	284.25
	60 minutes	285.46
	90 minutes	286.66
45˚C	40 minutes	285.46
	60 minutes	286.46
	90 minutes	287.65
50˚C	40 minutes	286.66
	60 minutes	287.86
	90 minutes	289.06

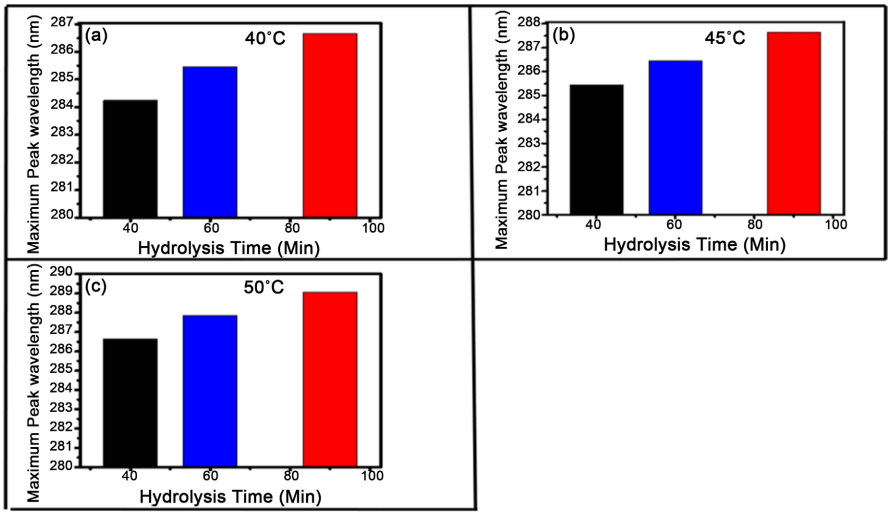

Figure 3. The peak position of the time dependence absorbance.

The peak absorbance (maximum wavelength) generally increased with hydrolysis time at all three temperatures. The redshift in the peak absorbance suggested structural changes or concentration variations in the substance as hydrolysis progressed. The rate of redshift varied depending on the temperature, with higher temperatures generally resulting in more rapid changes in absorbance and a greater redshift in the peak wavelength. (**Figure 2**, **Table 1**, **Figure 3**)

A red shift in the peak wavelength indicates a decrease in energy and an increase in the wavelength of light absorbed. In our research experiment, the observed redshift with increasing hydrolysis time suggests changes in the chemical structure and composition of the sample over time. As hydrolysis progresses, the chemical structure of the sample may change. This could be due to the breakdown of larger molecules into smaller ones or the formation of new chemical bonds [18]. These structural changes led to alterations in the electronic environment of the molecules, affecting the energy levels involved in absorption and resulting in a redshift. Over time, the concentration of the reactants and products in the solution

changed due to the progress of the hydrolysis reaction.

At higher temperatures, the rate of reaction typically increases due to the increased kinetic energy of the molecules. This accelerated the hydrolysis process, leading to faster structural changes and, consequently, a more pronounced red shift in peak wavelengths over shorter time intervals compared to lower temperatures. In summary, the observed red shift in peak wavelengths with increasing hydrolysis time at each temperature was attributed to a combination of structural changes, concentration effects, temperature effects, and the formation of intermediate species during the hydrolysis process. (Table 2, Figure 4)

Table 2. Peak intensities of time dependent absorption of CNC.

Temperature	Hydrolysis time (Minutes)	Peak intensity (a.u)
40˚C	40	0.1698
	60	0.5000
	90	1.0416
45˚C	40	0.447
	60	1.9703
	90	3.765
50˚C	40	2.323
	60	5.329
	90	6.024

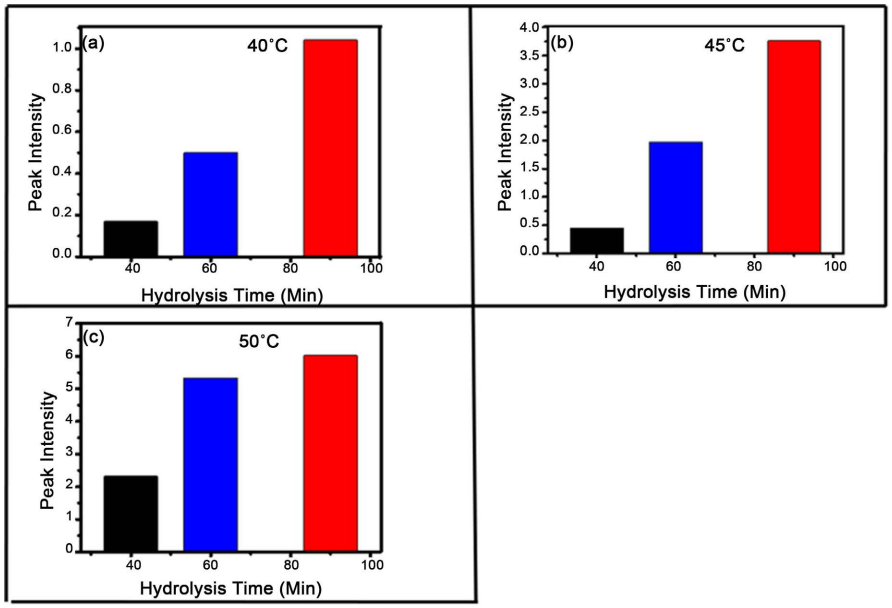

Figure 4. The peak intensities of the time dependent absorbance of CNC samples.

The absorption intensity of the samples increased with an increase in hydrolysis time; as the hydrolysis time increased, there was a notable increase in peak intensity at each time point. This suggests that more of the CNC was formed in the

solution as the hydrolysis progressed. The increase in intensity from 40 to 60 minutes is significant, and there is another substantial increase from 60 to 90 minutes. This indicates that the hydrolysis reaction might be accelerating or becoming more efficient over time, leading to a rapid accumulation of the absorbing species.

The rate of the hydrolysis reaction was higher in the later stages (60 to 90 minutes) compared to the initial stages (40 to 60 minutes). This could be due to various factors like the depletion of reactants, increased formation of catalysts, or the progression to a more favorable reaction pathway. The peak intensity values approached a saturation point as the hydrolysis time increased. It suggested that there might be a limit to crystallinity of the CNCs formed in the solvent, which indicated that the hydrolysis reaction might have reached equilibrium at longer times. (Figure 5, Table 3, Figure 6)

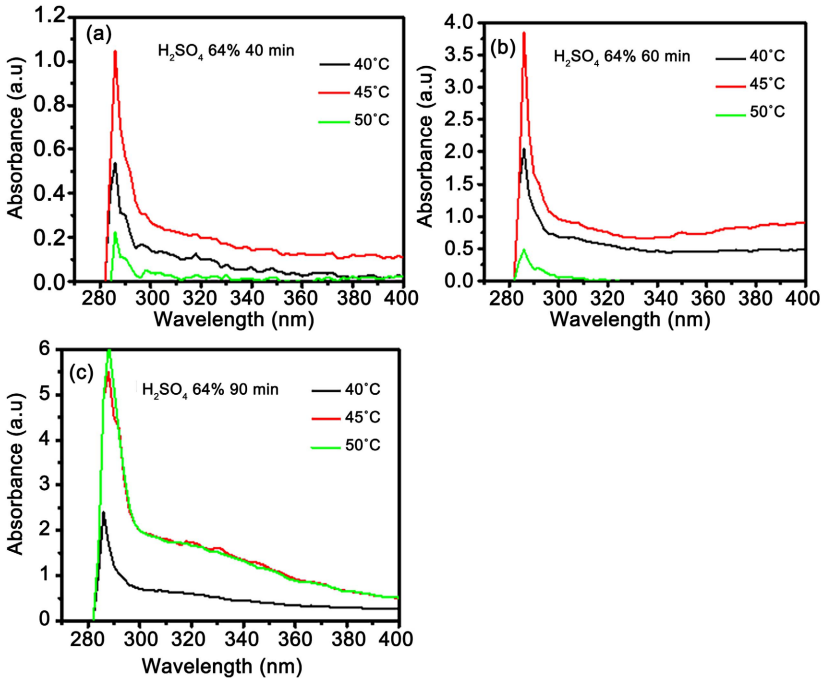

Figure 5. Absorbance spectra for CNC for temperature dependence hydrolysis.

Table 3. Peak position for temperature dependence absorption for CNC.

Hydrolysis time (Minutes)	Hydrolysis temperature	Maximum wavelength
40	40˚C	286.4128
	45˚C	286.118
	50˚C	285.8173
60	40˚C	286.117
	45˚C	285.817
	50˚C	285.216

Continued

	40˚C	288.2512
90	45˚C	287.920
	50˚C	286.117

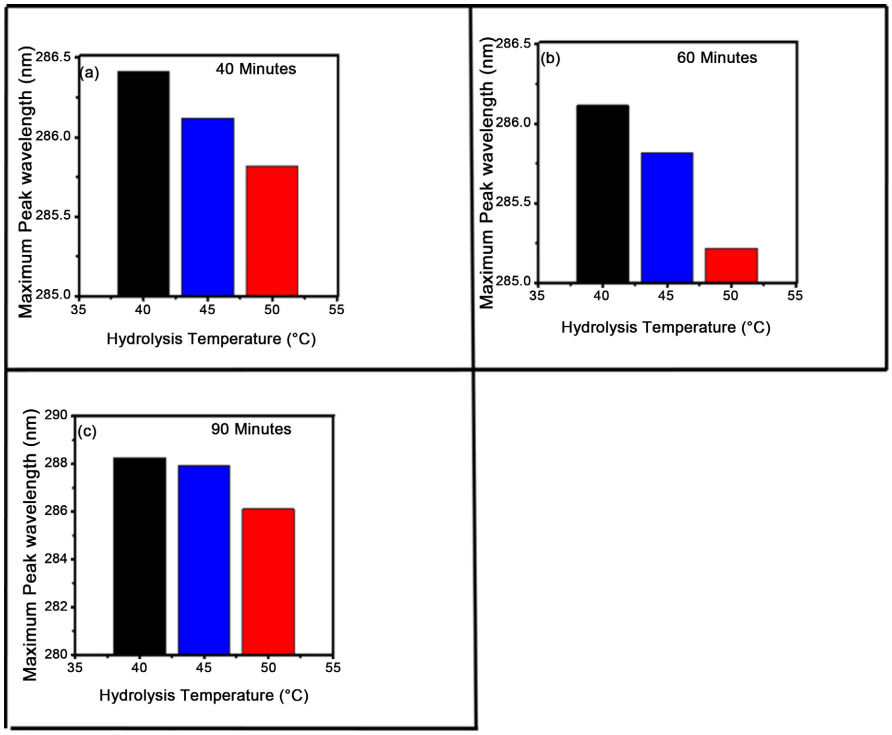

Figure 6. The peak of the temperature dependence absorbance of the CNC samples.

A blue shift in the peak wavelength indicated an increase in energy and a decrease in the wavelength of light absorbed. In the context of CNCs hydrolysis experiments with varying temperatures, the observed blue shift with increasing temperature was attributed to several factors. At higher temperatures, the rate of reaction typically increases due to increased molecular motion and kinetic energy. This accelerated rate of reaction leads to faster hydrolysis reaction and formation of CNCs, resulting in a shift towards shorter wavelengths (blue shift). Elevated temperatures also promoted the decomposition of certain compounds present in the sample. The breakdown of these compounds might lead to the formation of new absorbing species with different electronic transitions, resulting in a change in the absorption spectrum and a blue shift in the peak wavelength. (**Table 4**, **Figure 7**)

At 90 minutes of hydrolysis at 40˚C, the peak intensity was moderate. At 45˚C and 50˚C, Surprisingly, there was a substantial increase in peak intensity. This rise suggested that at extended hydrolysis times, higher temperatures might have promoted the formation of specific molecular structures or that enhance light absorption or emission at the maximum wavelength.

Table 4. Peak intensities of the temperature dependence absorbance for CNC.

Hydrolysis time (minutes)	Hydrolysis temperature (˚C)	Peak intensities (a.u)
40	40	1.048
	45	0.54
	50	0.223
60	40	3.860
	45	2.0434
	50	0.4681
90	40	2.4185
	45	5.5029
	50	6.126

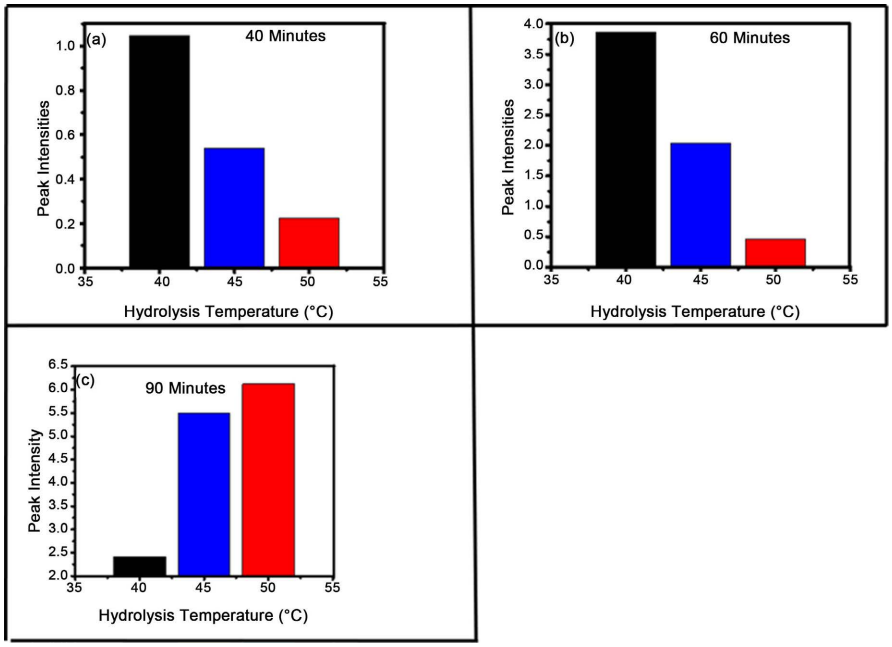

Figure 7. The peak intensities of the time dependence absorbance of CNC samples.

The shift in peak intensities with temperature at each hydrolysis time indicates that temperature had a significant impact on the molecular configurations, concentrations, and chemical compounds formed during hydrolysis. While higher temperatures generally result in decreased peak intensities, the relationship can change with longer hydrolysis times, where higher temperatures might induce conditions favoring increased light absorption or emission.

The variation in peak intensities with increasing temperature at various fixed hydrolysis times suggested that temperature plays a significant role in the hydrolysis of cellulose nanocrystals from rice husks using sulfuric acid. High temperatures generally accelerate chemical reactions due to increased molecular motion and kinetic energy. In this context, the hydrolysis of cellulose nanocrystals proceeded more rapidly at elevated temperatures, leading to a faster consumption of

the cellulose and a decrease in the concentration of CNCs, which was responsible for absorption leading to the observed peaks. This resulted in a decrease in peak intensities as the temperature increased. Elevated temperatures can also promote the thermal decomposition of cellulose and other compounds present in the rice husks [19]. The breakdown of these molecules reduced the overall concentration of the CNCs, contributing to the observed decrease in peak intensities at higher temperatures. (**Figure 8**, **Table 5**)

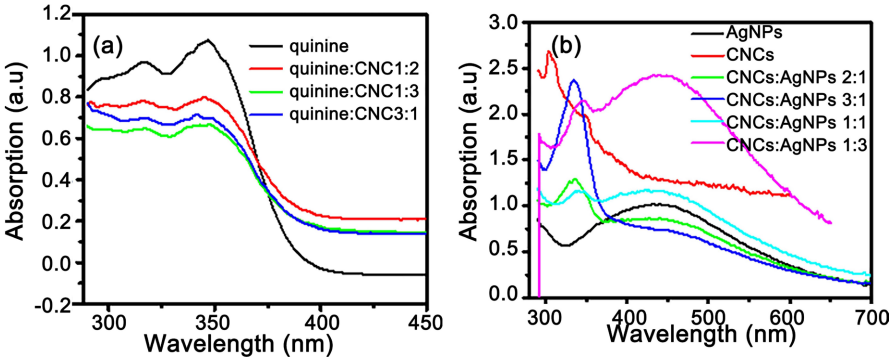

Figure 8. Absorbance spectra for (a) CNC AgNP composite and (b) CNC Quinine composite.

Table 5. Absorbance peaks and peak intensities of the CNC and its composites.

Sample	Ratio of CNC:AgNPs	Absorbance peak (nm)		Absorbance intensity (a.u)	
		CNCs	AgNPs	CNCs	AgNPs
AgNPs	0:1	-	438	-	1.0545
CNCs	1:0	290	-	2.6745	-
CNCs:AgNPs	2:1	337	444	1.2983	0.8583
CNCs:AgNPs	3:1	335	-	2.3666	-
CNCs:AgNPs	1:2	342	439	1.1591	1.1666
CNCs:AgNPs	1:3	347	443	2.1451	2.4091

A red shift typically refers to a shift in the wavelength of maximum absorbance towards longer wavelengths, which is indicative of changes in the electronic environment or interactions within the system. Based on the provided data, we can observe that as the ratio of AgNPs to CNCs increases, there is a red shift in the absorbance peak of CNCs. This shifts towards longer wavelengths. The red shift observed in the absorbance peak of cellulose nanocrystals (CNCs) upon interaction with silver nanoparticles (AgNPs) can be attributed to a multitude of factors. AgNPs are known for their surface plasmon resonance (SPR), which can interact with nearby molecules or nanoparticles like CNCs, inducing changes in their electronic environment. As AgNP concentration increases, enhanced particle aggregation occurs, altering the local environment around CNCs. This interaction facilitates electronic coupling between AgNPs and CNCs, affecting CNCs' energy levels and transitions. Additionally, changes in CNCs' surface chemistry due to

AgNP presence may contribute to the observed redshift. The complexity of these interactions underscores the importance of understanding nanoscale interactions in composite systems. Theoretical frameworks describing SPR and localized surface plasmon resonance (LSPR) provide insights into these phenomena, as do electromagnetic interaction studies and models on nanoparticle aggregation dynamics. Quantum mechanical calculations, such as density functional theory (DFT) simulations, offer a further understanding of the electronic structure and optical properties of these nanomaterials. By integrating experimental validation and computational modeling, researchers can deepen their comprehension of the mechanisms driving the observed red shift in CNC absorbance upon AgNP interaction, suggesting changes in the electronic structure or interactions between CNCs and AgNPs.

The slight redshift observed in the peaks of CNC quinine composite of ratio quinine to CNC of 3:1, with a wavelength of 348 nm, in contrast to the peak of quinine at 346 nm, suggests significant alterations in the electronic environment surrounding the quinine molecules upon their interaction with CNCs. One possible explanation for this shift is the interaction between the quinine molecules and the surface functional groups present in CNCs. Upon incorporation into the CNC matrix, quinine molecules may engage in various interactions, such as hydrogen bonding or π-π stacking with hydroxyl groups on the CNC surface. These interactions likely induce changes in the electronic structure of quinine molecules, ultimately leading to a redshift in the absorption peak observed in the UV-Vis spectra [20]. The observed blue shift in the fluorescence spectrum of the CNC (cellulose nanocrystals) quinine composites, particularly with ratios of 3:1 and 2:1, compared to pure quinine, can be attributed to several factors. The introduction of CNC into the quinine matrix alters the local environment around the quinine molecules. The surface chemistry of the CNC, including functional groups and surface defects, can interact with the quinine molecules, causing changes in their electronic structure and energy levels. This interaction may lead to a modification in the excited state properties of quinine, resulting in a shift in its fluorescence emission towards shorter wavelengths, hence the blue shift. The proximity of quinine molecules to the CNC surface can influence their electronic transitions. The confinement effect imposed by the nanostructure of CNC affects the spatial distribution of electronic states within the quinine molecules, altering their absorption and emission characteristics. This phenomenon is commonly observed in nanostructured materials, where quantum confinement effects lead to shifts in the energy levels of confined electronic states [21].

3.3. Thermal Properties of CNCs and AgNPs

In this study, the thermogravimetric analysis curves were used to determine the degradation and thermal stability of each material. The TGA analysis of cellulose nanocrystals and silver nanoparticle composite and cellulose nanocrystals and Quinine composite is represented in **Figure 9**.

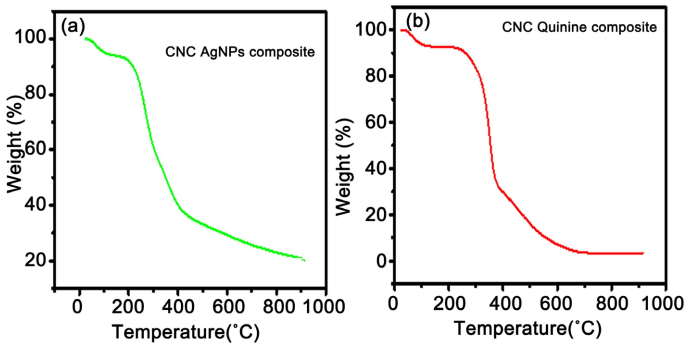

Figure 9. TGA Thermograms for (a) CNC AgNP composite and (b) CNC Quinine composite (right side) shows their TGA thermograms.

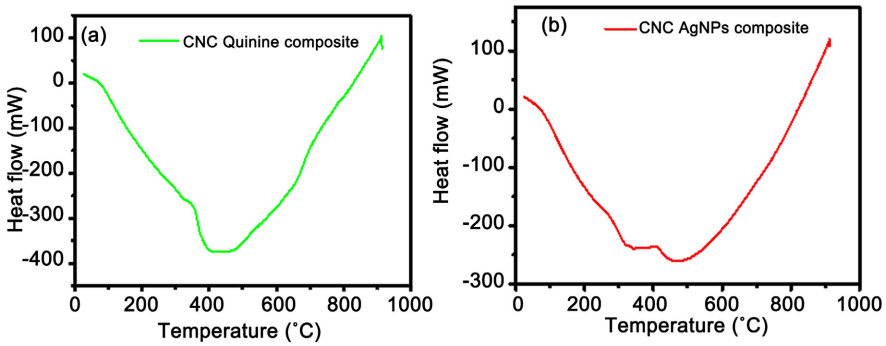

Figure 10. DSC thermograms for (a) CNC AgNP composite and (b) CNC Quinine composite.

The CNC AgNPs composite exhibits a first step weight loss of 6.0%, followed by a more significant second step weight loss of 72.7%, with a peak decomposition temperature of 212˚C. The initial weight loss in the first step is attributed to the evaporation of absorbed water and the release of volatile compounds. The substantial second step weight loss suggests the main degradation of the cellulose matrix, likely due to the breakdown of the cellulose backbone and the loss of the functionalized silver nanoparticles. The relatively moderate peak decomposition temperature indicates decent thermal stability, but it is lower than many other polymer composites, suggesting that the addition of AgNPs may reduce the overall thermal stability of the CNC composite. Literature supports that the incorporation of metal nanoparticles can alter the thermal decomposition pathway of cellulose-based materials, often leading to lower thermal stability due to the catalytic effect of the nanoparticles, which accelerate the degradation process [22].

In contrast, the CNC Quinine composite shows a first step weight loss of 5.75%, which is similar to that of the CNC AgNPs, indicating a similar initial moisture and volatile content. However, the second step weight loss is significantly higher at 86.1%, with a peak decomposition temperature of 235˚C. This higher peak temperature suggests better thermal stability compared to the CNC AgNPs composite. The increased second step weight loss is attributed to the more extensive degradation of the cellulose matrix and the quinine functional groups. The literature

indicates that the incorporation of organic compounds like quinine into cellulose nanocrystals can enhance the thermal stability of the composite due to the formation of more stable intermolecular interactions and possible cross-linking during the decomposition process [22]. The low melting point also facilitates recycling and reprocessing, enhancing sustainability by enabling the reuse of the material in various applications. Moreover, the composite's sensitivity to temperature can be useful in temperature-sensing applications, where changes in its properties at lower temperatures can provide valuable optical or physical feedback. The DSC curve for CNC Silver nanoparticle composite showed two endothermic peaks of heat flow as shown in **Figure 10**. For CNC AgNP composite, the first peak was observed around 345˚C, which represented the glass transition temperature. The onset temperature for the transition was 29.83˚C and the endset temperature was 911.68˚C. The second endothermic peak was observed at around 490˚C representing the melting point. The peak of decomposition was determined to be 482.52˚C. On the other hand, for CNC Quinine composite depicted one endothermic peak. The peak represented the combined glass transition temperature and melting temperature. The onset temperature for the transition was 28˚C and the end set temperature was 912˚C. The endothermic peak was observed at around 490˚C, representing the melting point. The peak of decomposition was determined to be 469.47˚C.

4. Conclusion

The delignification and bleaching process has proved to be essential steps in the isolation of cellulose and paving the way for hydrolysis and synthesis of the composites. Silver nanoparticles have proved to enhance the optical properties of CNC by enhancing thermal stability. The TGA/DSC spectroscopy has indicated that the CNC AgNP composite had a relatively lower thermally stability and agreed with the literature. The CNC AgNPs composite exhibits two distinct endothermic peaks: a glass transition at 345˚C and a melting temperature at 490˚C. The presence of two peaks indicates a complex thermal behavior where the composite undergoes a transition from a glassy to a rubbery state, followed by melting. In contrast, the CNC Quinine composite shows a single peak at 469˚C, representing both the glass transition and melting point, indicating a more straightforward thermal transition. UV-Vis spectroscopy has also demonstrated that The study has demonstrated that AgNP and Quinine modified the chemical, thermal and optical properties of CNC, placing it for potential application in several fields. This research has shown that CNC was extracted successfully and the optical signatures modified.

Acknowledgements

We, the authors, wish to acknowledge the Department of Physical Sciences, JOOUST, for availing of the equipment required for research. We also take this opportunity to thank our research collaborator, Prof. Martin Onani, from the

University of the Western Cape, Cape Town, South Africa, for FTIR tests and Mr. Godias Tumusiime, Faculty of Engineering, Busitema University, Uganda, for TGA and DSC analysis and all colleagues in SBPMAS-JOOUST, for their support and encouragements during the entire period of this work.

Conflicts of Interest

The authors have no conflict of interest to declare.

References

[1] Sarkar, A.N. (2013) Promoting Eco-Innovations to Leverage Sustainable Development of Eco-Industry and Green Growth. *European Journal of Sustainable Development*, **2**, 171-224.

[2] Xu, S., Girouard, N., Schueneman, G., Shofner, M.L. and Meredith, J.C. (2013) Mechanical and Thermal Properties of Waterborne Epoxy Composites Containing Cellulose Nanocrystals. *Polymer*, **54**, 6589-6598. https://doi.org/10.1016/j.polymer.2013.10.011

[3] Roy, S. and Das, T.K. (2015) Plant Mediated Green Synthesis of Silver Nanoparticles. *International Journal of Plant Biology & Research*, **3**, 1044-1055.

[4] Ghosh, S.K. and Pal, T. (2007) Interparticle Coupling Effect on the Surface Plasmon Resonance of Gold Nanoparticles: From Theory to Applications. *Chemical Reviews*, **107**, 4797-4862. https://doi.org/10.1021/cr0680282

[5] Singh, S.S., Salem, D.R. and Sani, R.K. (2021) Spectroscopy, Microscopy, and Other Techniques for Characterization of Bacterial Nanocellulose and Comparison with Plant-Derived Nanocellulose. In: Das, S. and Dash, H.R., Eds., *Microbial and Natural Macromolecules*, Elsevier, 419-454. https://doi.org/10.1016/b978-0-12-820084-1.00018-1

[6] Monnier, G.F. (2018) A Review of Infrared Spectroscopy in Microarchaeology: Methods, Applications, and Recent Trends. *Journal of Archaeological Science: Reports*, **18**, 806-823. https://doi.org/10.1016/j.jasrep.2017.12.029

[7] Agidi, R. (2021) Synthesis and Characterization of Iron Oxide from Clay Ore for Biomedical Applications. Ashesi University, 84 p. http://hdl.handle.net/20.500.11988/689

[8] Zhong, Z., Peng, F., Ying, L., Yu, G., Huang, F. and Cao, Y. (2021) Ternary Organic Photodiodes with Spectral Response from 300 to 1200 nm for Spectrometer Application. *Science China Materials*, **64**, 2430-2438. https://doi.org/10.1007/s40843-020-1639-x

[9] Robinson, J., Binner, E., Vallejo, D.B., Perez, N.D., Al Mughairi, K., Ryan, J., *et al.* (2022) Unravelling the Mechanisms of Microwave Pyrolysis of Biomass. *Chemical Engineering Journal*, **430**, Article ID: 132975. https://doi.org/10.1016/j.cej.2021.132975

[10] Gałko, G. and Sajdak, M. (2022) Trends for the Thermal Degradation of Polymeric Materials: Analysis of Available Techniques, Issues, and Opportunities. *Applied Sciences*, **12**, Article 9138. https://doi.org/10.3390/app12189138

[11] Teh, J.S., Teoh, Y.H., How, H.G. and Sher, F. (2021) Thermal Analysis Technologies for Biomass Feedstocks: A State-of-the-Art Review. *Processes*, **9**, Article 1610. https://doi.org/10.3390/pr9091610

[12] Lu, S., Ma, T., Hu, X., Zhao, J., Liao, X., Song, Y., *et al.* (2021) Facile Extraction and

Characterization of Cellulose Nanocrystals from Agricultural Waste Sugarcane Straw. *Journal of the Science of Food and Agriculture*, **102**, 312-321. https://doi.org/10.1002/jsfa.11360

[13] Kaabipour, S. and Hemmati, S. (2021) A Review on the Green and Sustainable Synthesis of Silver Nanoparticles and One-Dimensional Silver Nanostructures. *Beilstein Journal of Nanotechnology*, **12**, 102-136. https://doi.org/10.3762/bjnano.12.9

[14] Pavitha P.A., Suma Mahesh, S., Sumi, V.S. and Rijith, S. (2024) Insight to the Batch Reactor Design and Sorption Potential Profiling of Polymer Grafted Chitosan Embedded Silanated Halloysite for Th(IV) Recovery from Aqueous System. *Colloids and Surfaces A*: *Physicochemical and Engineering Aspects*, **689**, Article ID: 133646. https://doi.org/10.1016/j.colsurfa.2024.133646

[15] Dai, H., Zhang, Y., Ma, L., Zhang, H. and Huang, H. (2019) Synthesis and Response of Pineapple Peel Carboxymethyl Cellulose-G-Poly (Acrylic Acid-Co-Acrylamide)/Graphene Oxide Hydrogels. *Carbohydrate Polymers*, **215**, 366-376. https://doi.org/10.1016/j.carbpol.2019.03.090

[16] Frone, A.N., Batalu, D., Chiulan, I., Oprea, M., Gabor, A.R., Nicolae, C., *et al.* (2019) Morpho-Structural, Thermal and Mechanical Properties of PLA/PHB/Cellulose Biodegradable Nanocomposites Obtained by Compression Molding, Extrusion, and 3D Printing. *Nanomaterials*, **10**, Article 51. https://doi.org/10.3390/nano10010051

[17] Dong, Y., Bi, J., Zhu, D., Meng, D., Ming, S., Guo, W., *et al.* (2019) Functionalized Cellulose with Multiple Binding Sites for a Palladium Complex Catalyst: Synthesis and Catalyst Evaluation in Suzuki-Miyaura Reactions. *Cellulose*, **26**, 7355-7370. https://doi.org/10.1007/s10570-019-02568-w

[18] Huang, C., Jiang, X., Shen, X., Hu, J., Tang, W., Wu, X., *et al.* (2022) Lignin-Enzyme Interaction: A Roadblock for Efficient Enzymatic Hydrolysis of Lignocellulosics. *Renewable and Sustainable Energy Reviews*, **154**, Article ID: 111822. https://doi.org/10.1016/j.rser.2021.111822

[19] Hafid, H.S., Omar, F.N., Zhu, J. and Wakisaka, M. (2021) Enhanced Crystallinity and Thermal Properties of Cellulose from Rice Husk Using Acid Hydrolysis Treatment. *Carbohydrate Polymers*, **260**, Article ID: 117789. https://doi.org/10.1016/j.carbpol.2021.117789

[20] Zhang, Z., Chen, K., Tang, K., Chen, K., Li, R., Sun, X., *et al.* (2023) Quinine-fabricated Surface-Enhanced Raman Spectroscopy Chiral Sensing Platform Enables Simultaneous Enantioselective Discrimination and Identification of Aliphatic Amino Acids. *Analytical Chemistry*, **95**, 4923-4931. https://doi.org/10.1021/acs.analchem.2c04839

[21] Kambhampati, P. (2021) Nanoparticles, Nanocrystals, and Quantum Dots: What Are the Implications of Size in Colloidal Nanoscale Materials? *The Journal of Physical Chemistry Letters*, **12**, 4769-4779. https://doi.org/10.1021/acs.jpclett.1c00754

[22] D'Acierno, F., Hamad, W.Y., Michal, C.A. and MacLachlan, M.J. (2020) Thermal Degradation of Cellulose Filaments and Nanocrystals. *Biomacromolecules*, **21**, 3374-3386. https://doi.org/10.1021/acs.biomac.0c00805